

# Evaluating the Seismic Performance of Deep Soil Mixing: The Role of Motion Intensity in Improved Soil Response

Antania Hanjani<sup>1</sup>, Yuamar I. Basarah<sup>2</sup>, dan Wayan Sengara<sup>3</sup>

<sup>1</sup>Department of Civil Engineering, Faculty of Civil and Environmental Engineering, Institut Teknologi Bandung, Bandung,

*e-mail:* [antaniaa80@gmail.com](mailto:antaniaa80@gmail.com)

<sup>2</sup>Department of Civil Engineering, Faculty of Civil and Environmental Engineering, Institut Teknologi Bandung, Bandung,

*e-mail:* [yuamarbasarah@itb.ac.id](mailto:yuamarbasarah@itb.ac.id)

<sup>3</sup>Department of Civil Engineering, Faculty of Civil and Environmental Engineering, Institut Teknologi Bandung, Bandung,

*e-mail:* [wayansengara@itb.ac.id](mailto:wayansengara@itb.ac.id)

## ABSTRACT

Liquefaction during earthquake shaking can reduce the shear strength and bearing capacity of soils supporting the backfill system. Deep Soil Mixing (DSM) is a ground improvement method used to mitigate liquefaction, and numerous studies have demonstrated its effectiveness in reducing shear stress and excess pore water pressure generation under seismic loading. However, most studies have not considered the effect of seismic motion intensity on improved ground performance. This study evaluates the influence of seismic loading intensity on the seismic response of DSM-improved soil using two-dimensional (2D) finite element analysis with a dynamic-with-consolidation approach that accounts for pore pressure dissipation during seismic loading. A parametric study was conducted to assess the effects of different DSM configurations, defined by soil improvement ratios and seismic motion intensity, on excess pore pressure reduction. The results indicate that the effectiveness of DSM in reducing liquefaction potential decreases under high-intensity motion; however, additional confining pressure from reinforced backfill provides further resistance against liquefaction. Moreover, increasing motion intensity leads to greater deformation and higher pore pressure ratio ( $R_u$ ), while higher soil improvement ratios result in greater reduction of liquefaction potential.

Keywords: Soil Improvement; Soil-Structure Interaction; Seismic Load; 2D Dynamic Effective Analysis

## 1. INTRODUCTION

Geographically, Indonesia is located at the meeting point of three world plates, namely the Eurasian, Australian and Pacific plates. The collision between these three plates makes Indonesia prone to earthquakes. Based on historical earthquake data in and around Indonesia from 1907 to August 2016, with a magnitude ( $M_w$ )  $\geq 4.5$ , approximately 51,855 earthquakes have occurred. This data has been collected by Pusat Studi Gempa Nasional (PuSGeN) from various sources. Susceptibility to earthquakes cannot be separated from the potential for liquefaction in saturated soil. The liquefaction that occurs can reduce the strength of the soil, causing it to behave more like a liquid.

Several studies, including those by Tsutomu Namikawa et al. (2007) and Raymajhi et al. (2015), have examined the effectiveness of Deep Soil Mixing (DSM) grids for mitigating liquefaction. However, most of these studies considered only limited seismic motions and did not account for the effect of varying motion intensities on DSM performance. This study investigates the effectiveness of DSM grid improvement at different improvement ratios under various seismic loading characteristics. The performance of DSM in reducing liquefaction is evaluated based on changes in excess pore pressure ratio ( $R_u$ ) and lateral deformation.

## 2. METHODS

The effectiveness of DSM in reducing liquefaction potential is evaluated based on the reduction of pore water pressure ratio ( $R_u$ ) in the surrounding soils. The analysis employs DeepSoil software to simulate one-dimensional (1D) wave propagation to the surface and PLAXIS to simulate the two-dimensional (2D) model. Ground motion outputs at each depth generated by DeepSoil serve as the basis for calibration to determine the Hardening Soil Small (HSS) parameters in PLAXIS. Liquefied soils are analyzed using the effective stress approach with the PM4SAND model. The modeling adopts a dynamic-with-consolidation approach to account for pore water pressure dissipation during loading. This approach is considered to more accurately represent field conditions and has been verified to align well with mini-scale experimental results.

### Soil Condition and Deep Soil Mixing properties

In this study, the primary data used as the basis for analysis, including the data of soil, structure, and earthquake. Soil data, as listed in Table 1, are generated data that have been adjusted to the soil characteristics required in this research, the data are assumed to be in the site class SE.

**Table 1. Soil Properties**

Layer	Soil Type	Depth (m)			NSPT (blows/30 cm)	$\gamma$ (kN/m <sup>3</sup> )	$\phi'$ (°)	Drained Modulus E' (kPa)	V <sub>s</sub> (m/s)	G <sub>max</sub> (kPa)
Layer 1	Loose sand	0	-	10	5	15	28.77	7000	149.43	34143.84
Layer 2	Med Dense Sand	10	-	22	17	16.25	36.18	17000	228.77	86692.97
Layer 3	Dense Sand	22	-	28	29	16.25	41.13	45000	275.5	125724.6
Layer 4	Very Dense Sand	28	-	40	44	18.63	46.03	58800	318.51	192661.1
Layer 5	Very Dense Sand	40	-	100	60	20	50.4	70000	354.81	256661.8

The effective stress analysis will be conducted on liquefied soil, which will be modeled using the PM4SAND parameters proposed by Boulanger and Ziotopoulou (2015). The parameters used are obtained from calibration with centrifuge tests on soil with a 40% density ratio, conducted by Nuques (2017) for Nevada Sand. Other parameters are set to their default values as suggested by Boulanger (2015). The parameters are provided in

Table 2:

Table 2. PM4SAND Soil Properties

Parameter	Value	Parameter	Value
$\gamma_{\text{unsat}}$ (kN/m <sup>3</sup> )	14.5	$\gamma_{\text{sat}}$ (kN/m <sup>3</sup> )	16
$e_0$	0.68	$D_{r0}$	0.4
$G_0$	550	$h_{p0}$	0.05
$p_A$ (kPa)	101.3	$e_{\text{max}}$	0.8
$e_{\text{min}}$	0.5	$n_b$	0.5
$n_d$	0.1	$\phi_{cv}$ (°)	33
$\nu$	0.3	$Q$	10
$R$	1.5	Post Shake	1
$k_x$ (m/day)	8.64	—	—

The properties of DSM in Table 3 are derived from the FHWA-HRT-13-046 manual. The DSM model is represented as a composite material with stiffness values adjusted based on the surrounding soil. In this study, two replacement ratios, Ar 16% and Ar 30%, will be examined to observe their effects on liquefaction reduction.

**Table 3. Deep Soil Mixing Properties**

Parameter	Value	Parameter	Value
$\gamma_{\text{unsat}}$	19	$\gamma_{\text{sat}}$	20
$e_0$	0.5	$E_{28}$ (kPa)	$9.00 \times 10^5$
$\nu$	0.2	$f_{c,28}$ (kPa)	0.4
$f_{c0n}$	550	$f_{cfn}$	0.05
$f_{cun}$	101.3	$G_{c,28}$ (kN/m)	0.8
$\phi_{\text{max}}$ (°)	0.5	$\psi$ (°)	0.5
$Y_{fc}$	0.1	$f_{t,28}$ (kPa)	33
$f_{tun}$	0.3	$G_{t,28}$ (kPa)	10
$Y_{ft}$	1.5	—	—

## Ground Motion

In this study, the earthquake mechanism to be examined is limited to shallow crustal, with difference intensity and frequency content. The earthquake intensities used in this study are 0.5 g for high-intensity earthquakes and 0.3 g for moderate-intensity earthquakes. The example of input ground motion is shown in Figure 1 as follows:

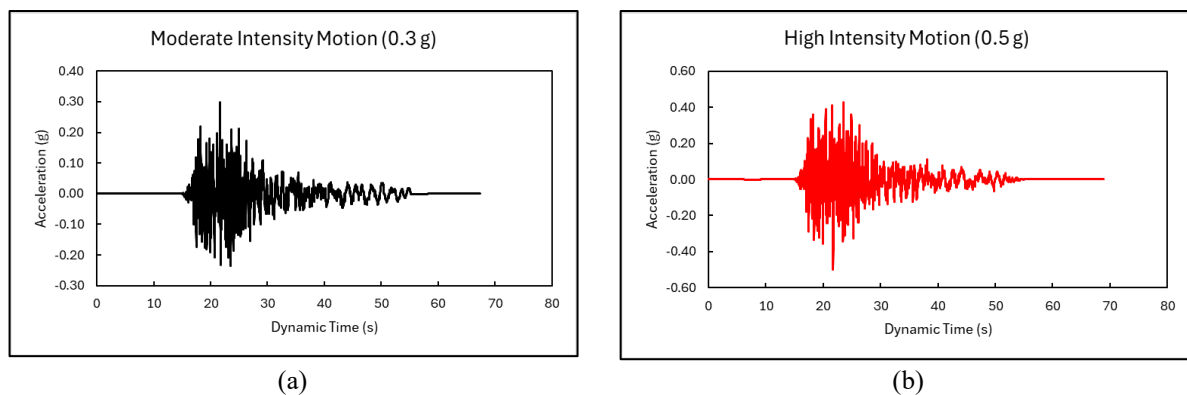


**Figure 1. Ground motion for different intensity (a) 0.3 g (b) 0.5 g**

## Development of Numerical Model

Verification of one-dimensional (1D) wave propagation in DEEPSOIL was conducted prior to developing the two-dimensional (2D) model to account for the nonlinear behavior of the soil and ensure that the input motion used in PLAXIS accurately represents the actual ground response. The propagation in DEEPSOIL was modeled using the GQ/H model with non-Masing reloading and unloading behavior, while the  $G/G_{\text{max}}$  and damping ratio curves were referenced from Darendeli (2001). The calibration process involved adjusting the Rayleigh damping in PLAXIS to match the motion output from DEEPSOIL at various depths. This was achieved by comparing the Peak Spectral Acceleration (PSA) values at the midpoint of each soil layer. The results of this calibration, illustrated in Figure 2 and Figure 3, yielded modified  $\gamma_{0.7}$  and  $E_{ur}$  values, which were then used as input parameters for the Hardening Soil Small (HSS) model in PLAXIS. These calibrated parameters, summarized in Table 4, were subsequently applied in the 2D model to represent the soil's dynamic behavior more accurately.

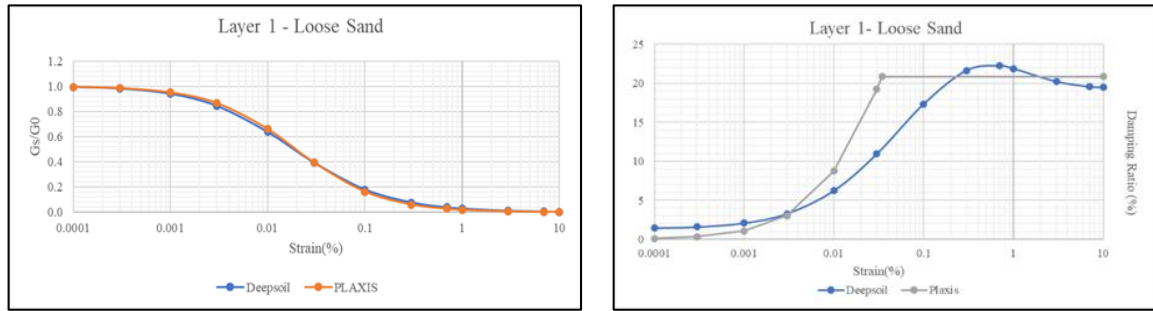


Figure 2. Ground Motion Input for Various

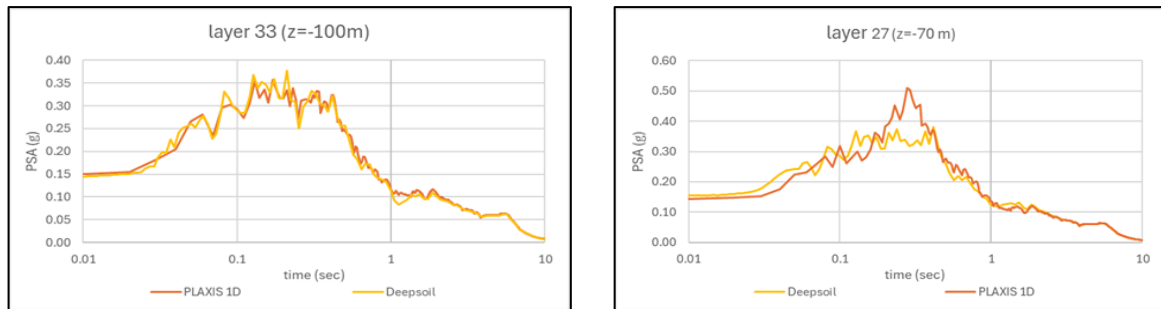


Figure 3. Ground Motion Input for Various

Table 4. Hysteretic damping parameter

Layer	Soil Type	D1 (%)	D2(%)	f1 (Hz)	f2 (Hz)	E50=E <sub>ed</sub> (kPa)	E <sub>ur</sub> (kPa)	G <sub>o</sub> (kPa)	$\gamma_{0.7}$
Layer 1	PM4Sand	1	1	0.2	0.6				
Layer 2	Dense Sand	1.5	1.5	0.2	0.75	17e3	51e3	125e3	0.07e-3
Layer 3	Dense Sand	2	2	0.2	0.75	45e3	135e3	150e3	0.15e-3
Layer 4	Very Dense Sand	2	2	0.2	0.75	58.8e3	176.4e3	250e3	0.1e-3
Layer 5	Very Dense Sand	1	1	0.2	0.75	70e3	210e3	650e3	0.1e-3

The two-dimensional (2D) analysis was performed using PLAXIS software with a dynamic-with-consolidation approach, conducted in two stages. In the first stage, when seismic motion remains significant, the post-shake parameter is deactivated (post shake = 0). In the second stage, after the seismic motion ceases, the post-shake parameter is activated (post shake = 1) and the simulation is extended for an additional 100 to 200 seconds. This setup allows the model to capture post-seismic soil behavior, including pore water pressure dissipation and subsequent ground response stabilization.

Due to limitations in representing the DSM grid geometry, the DSM will be modeled equivalently to capture the actual soil response at the center of the grid. The equivalent modeling approach is applied to grids of 8×5 m and 16×8 m, corresponding to area improvement ratios of 30% and 15%, respectively. Soil behavior is analyzed along the representative cross-sections AA (for the 8×5 m grid) and BB (for the 16×8 m grid), as illustrated in Figure 4. To optimize computational efficiency, the 2D model is developed using a unit grid geometry represented under unit cell model, as shown in Figure 5.

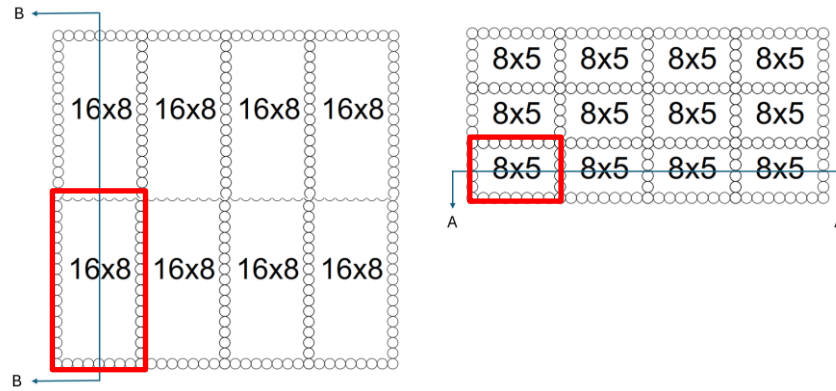


Figure 4. Layout of DSM grid configuration

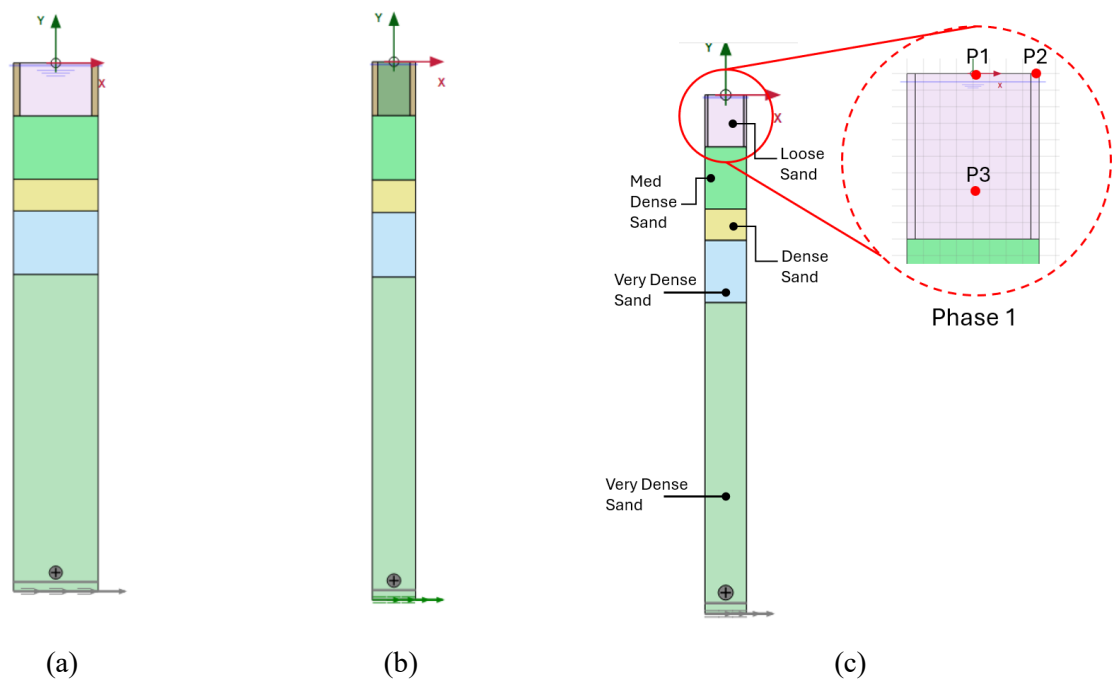


Figure 5. 2D unit cell model; (a) Ar 15%; (b)Ar 30%; and (c) monitoring points in PLAXIS 2D.

Variables considered in this analysis include seismic mechanisms, earthquake intensity, soil improvement ratio, and confining pressure on the improved soil as mention in Table 5.

Table 5. Parametric Study

Intensity	Frequency	Ar Ratio (%)
High (0.3 g)	High	0
		15
		30
Low (0.12 g)	High	0
		15
		30

### 3. NUMERICAL RESULTS

There are three observation points, P1 to P3, used in this study. P1 (0,0) and P2 (3.5,0) are nodal points designated for analyzing the deformation of the structure, while P3 (0,-6.7) is a stress point used to evaluate the response of the pore water pressure ratio. The locations of points P1 through P3 can be seen in Figure 5c

### Effects of Replacement ratio

In this study, the values of Ar 0% (without improvement), Ar 15%, and Ar 30% will be compared under specific confinement conditions and earthquake intensity. The effect of replacement ratio under the same motion intensity will be presented in Figure 6, from points a to d.

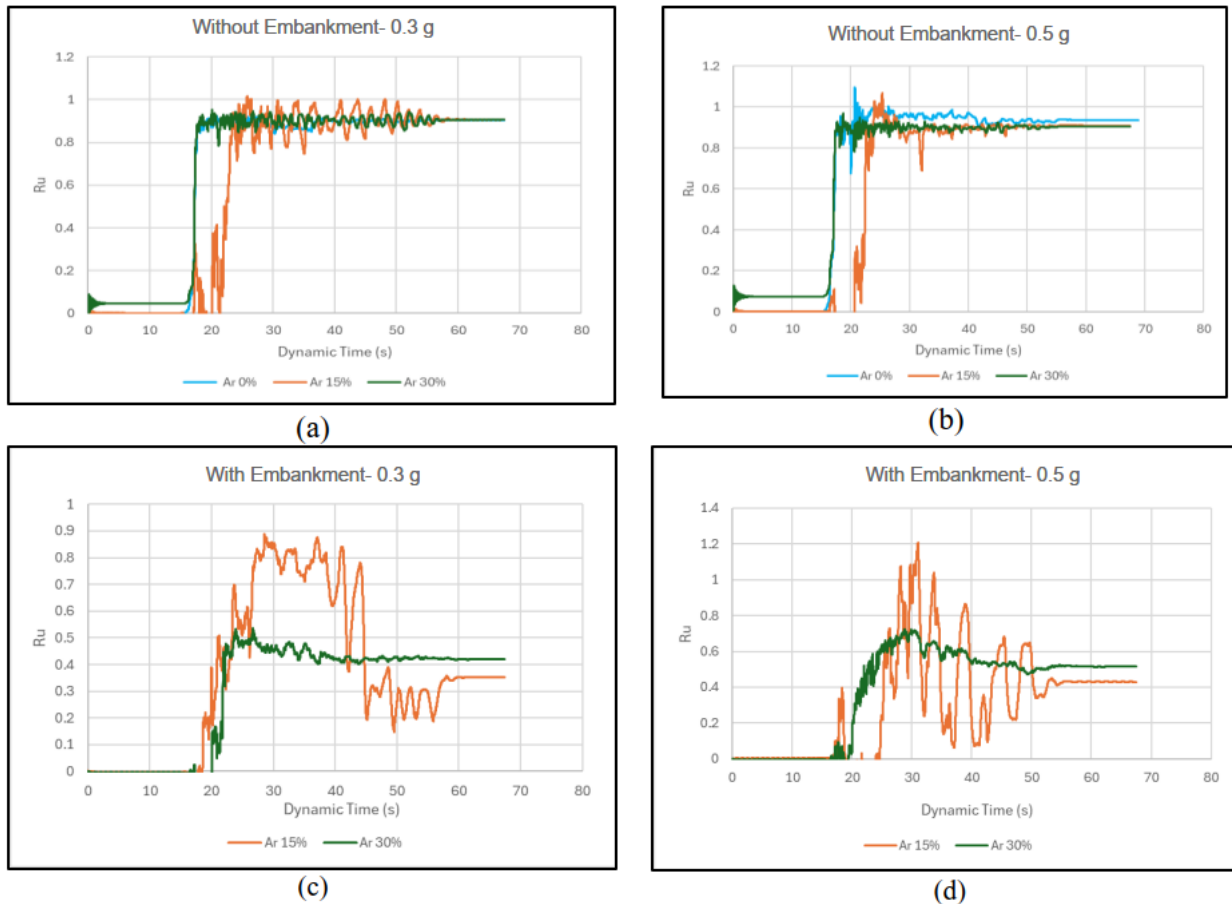


**Figure 6. Replacement ratio effect on various intensity and confinement condition (a) without embankment condition with 0.3 g motion, (b) without embankment condition with 0.3 g motion, (c) With Embankment loadings with 0.3 g motion, (d) With Embankment loadings with 0.5 g motion**

Under MSE embankment conditions without the MSE wall and at moderate earthquake intensity (0.3g), a 15% replacement ratio was found to be more effective in mitigating liquefaction effects. This is evidenced by the longer time required for excess pore pressure to develop and trigger liquefaction, as shown in point (a). The likely reason is that the 15% replacement ratio results in a greater volume of untreated soil between DSM columns. Although untreated soil is more prone to liquefaction, the larger void area may dissipate and redistribute seismic energy more gradually, thereby slowing excess pore pressure buildup and delaying the onset of liquefaction. This finding suggests that for moderate seismic conditions, a lower replacement ratio can provide a balance between stiffness contrast and energy absorption, resulting in improved overall ground performance.

Under MSE embankment conditions with the MSE wall, neither moderate nor high-intensity earthquakes led to liquefaction. The presence of the MSE wall provides additional confinement, enhancing the stability of the improved soil mass. However, under moderate seismic loading, the 15% replacement ratio again showed superior performance, indicated by lower  $R_u$  values in point (a) and a delayed excess pore pressure response in point (b). These results highlight that, in reinforced embankment systems, increasing the stiffness through a higher replacement ratio does not necessarily yield proportional benefits; instead, an optimal replacement ratio—such as 15% in this case—can achieve more efficient mitigation by improving energy dissipation and maintaining favorable stress redistribution within the treated zone.

### Effects of Motion Intensity

The effects of shallow crustal earthquake intensities of 0.3g and 0.5g were compared under specific confinement conditions and replacement ratios, as illustrated in Figure 7 (points a–d). In both the with and without MSE

embankment conditions, the higher earthquake intensity of 0.5g generated greater excess pore pressure ratios ( $R_u$ ) than the 0.3g motion, indicating a stronger tendency toward liquefaction with increasing seismic demand. However, as shown in point (b), the 30% replacement ratio proved more effective in mitigating liquefaction under the higher intensity (0.5g) scenario. This improvement is attributed to the increased stiffness and reduced deformability of the treated ground, which help limit shear strain accumulation and restrain excess pore pressure generation. These findings suggest that while lower replacement ratios may perform adequately under moderate shaking, higher replacement ratios become necessary to maintain stability and minimize liquefaction potential under more severe seismic loading.

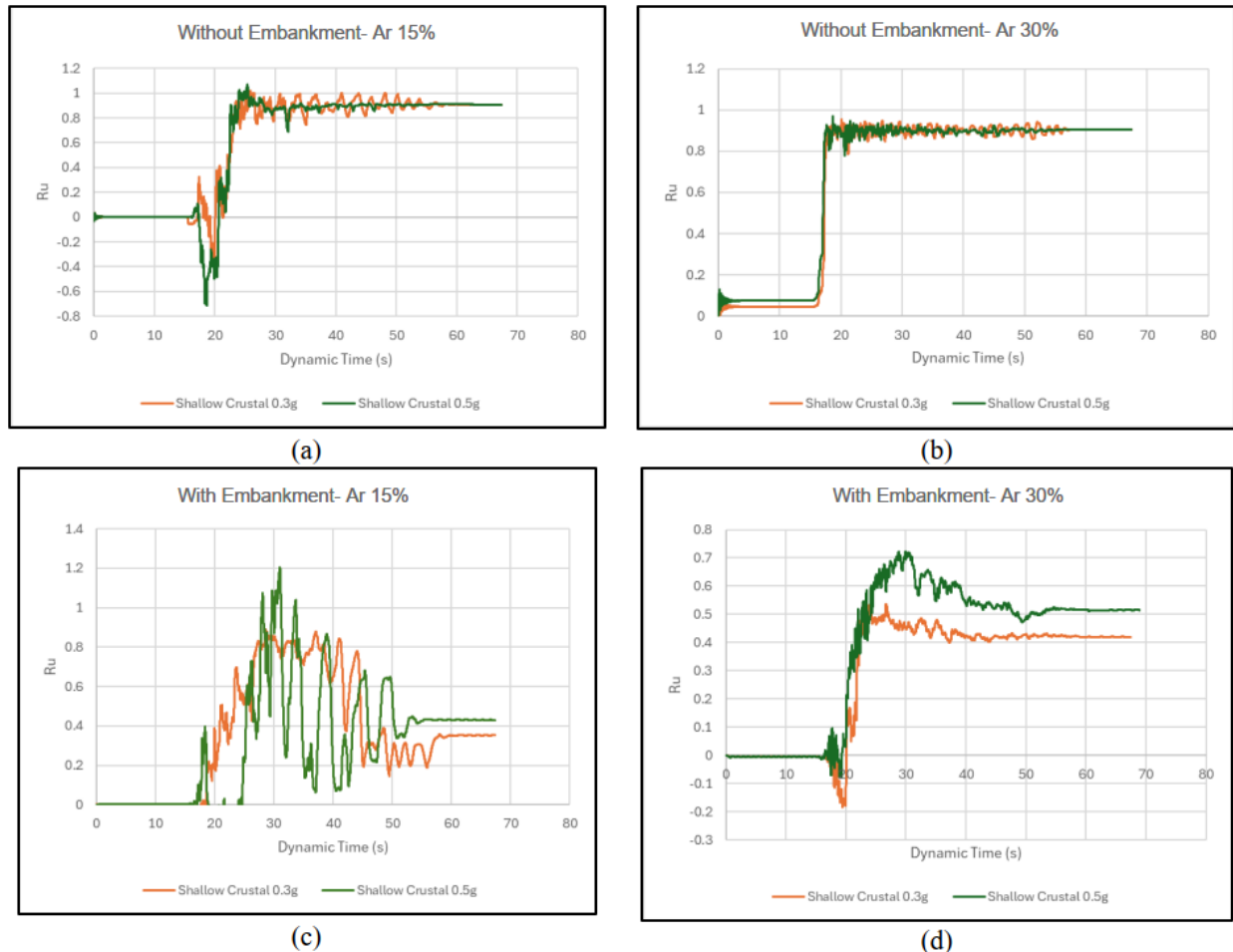


**Figure 7. Intensity motion effect on various replacement ratio and confinement condition: (a) without embankment condition with  $Ar=15\%$ , (b) without embankment condition with  $Ar=30\%$ , (c) Embankment loadings with  $Ar=15\%$ , (d) Embankment loadings with  $Ar=30\%$ ,**

### Effects of Confining Pressures (Embankment)

The effects of confining pressure (with the presence of an MSE Wall) and without an MSE Wall will be compared for specific intensities and replacement ratios. The effect of confining pressure will be presented in Figure 8, from points (a) to (d). The confining effect of the MSE Wall significantly reduces the  $R_u$  values for each intensity and specific improvement area. This occurs because the overburden pressure increases due to the embankment, which in turn helps to decrease the  $R_u$  values.

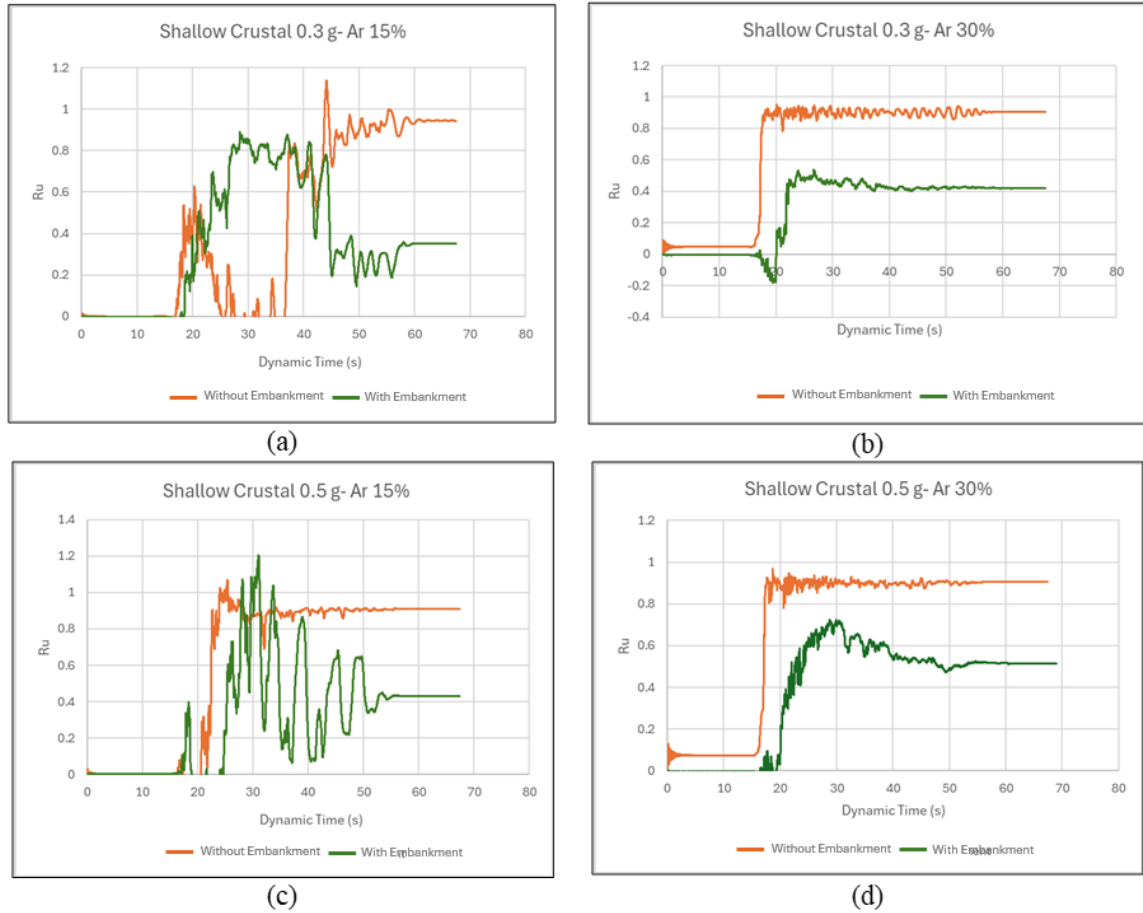


Figure 8. Confining Pressure effect on various replacement ratio and confinement condition: (a) Intensity 0.3g with Ar=15%, (b) Intensity 0.3g with Ar=30%, (c) Intensity 0.5g with Ar=15%, (d) Intensity 0.5g with Ar=30%

The effects of the replacement ratio and earthquake intensity were also evaluated in terms of lateral deformation of the MSE embankment. Figure 9 shows that, in general, an increase in the replacement ratio reduces the relative lateral deformation. This implies that the the DSM increased the stiffness of the embankment system and hence limit the deformation.

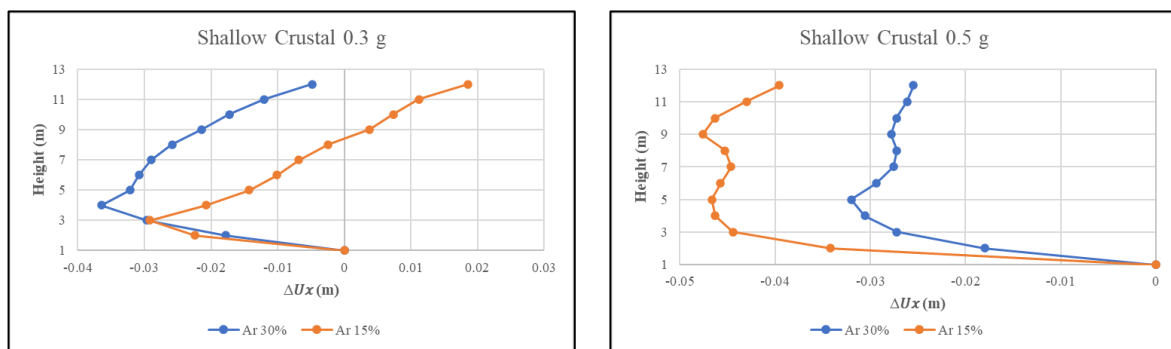


Figure 9. Deformation due to Replacement ratio Effect

The lateral deformation was also observed to be increased with the motion intensity. Figure 10 shows that the lateral deformation for 0.5g motion intensity can increase up to 3 times of lateral deformation obtained from 0.3g case with total relative deformation of about 5 cm. For the case of 30% replacement ratio, the maximum relative deformation was about 3.5 cm.



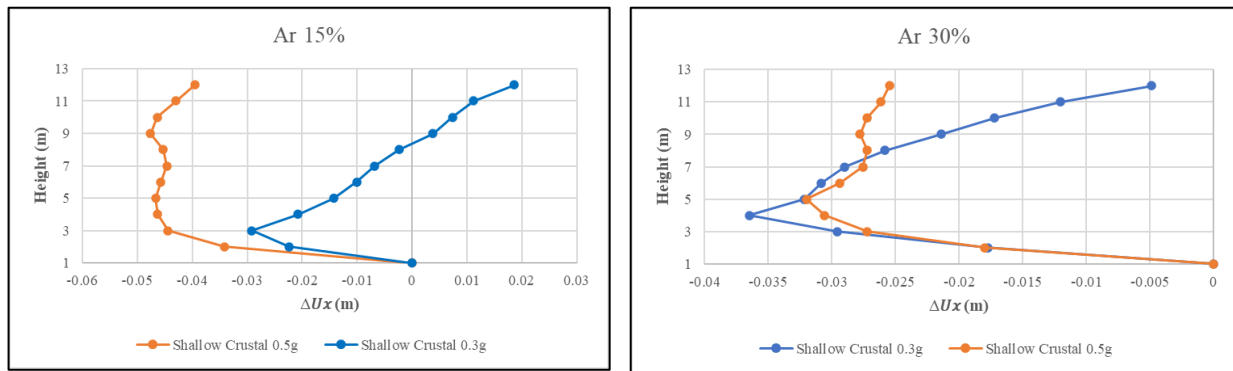


Figure 10. Deformation due to Earthquake Intensity Effect

## 4. DISCUSSION

The unit grid DSM model shows an insignificant change in the  $R_u$  value at the central portion of the model, which is not directly improved by DSM columns. This limited variation is likely a result of the plane strain assumption, which constrains lateral deformation and pore pressure redistribution within the 2D framework. To better capture the actual soil behavior and stress transfer between treated and untreated zones, a more realistic three-dimensional (3D) analysis and additional cross-sectional evaluations are required. Nevertheless, the analysis confirms that increasing overburden pressure is effective in reducing liquefaction effects by enhancing confining stress and suppressing excess pore pressure generation. Therefore, incorporating existing structural loads or embankment effects into future models is recommended to achieve more representative and less conservative predictions of soil response under seismic loading.

## 5. CONCLUSION

1. The application of the DSM grid model does not significantly reduce excess pore pressure in the untreated zones between columns; however, at specific motion intensities and replacement ratios, DSM demonstrates measurable effectiveness in mitigating liquefaction potential. This is evident in Figure 6 and Figure 7, where the optimized replacement ratio shows delayed pore pressure buildup and reduced  $R_u$  values under seismic loading.
2. The presence of additional overburden pressure from existing structures effectively reduces the excess pore pressure ratio ( $R_u$ ), as illustrated in Figure 8. This indicates that increased confinement enhances soil stability and mitigates the onset of liquefaction compared to the without embankment condition.
3. Increasing the replacement ratio leads to a reduction in lateral deformation, whereas higher seismic motion intensity results in greater deformation. This relationship, presented in Figure 9 and Figure 10, confirms that both the degree of soil improvement and the intensity of seismic loading play critical roles in controlling the lateral displacement behavior of DSM-improved ground.

## 6. REFERENCES

- Badan Standardisasi Nasional. (2017). *SNI 1726:2019 Tata Cara Perencanaan Ketahanan Gempa untuk Struktur Bangunan Gedung dan Nongedung*. Jakarta: Badan Standardisasi Nasional.
- Boulanger, R. W., and Ziotopoulou, K. (2013). "Formulation of a sand plasticity plane-strain model for earthquake engineering applications." *Journal of Soil Dynamics and Earthquake Engineering*, Elsevier, 53, 254-267, 10.1016/j.soildyn.2013.07.006.
- Federal Highway Administration (FHWA). (2013). *Ground Improvement Methods: Volume I – Deep Mixing Method* (FHWA-HRT-13-046). U.S. Department of Transportation, Federal Highway Administration, Office of Infrastructure Research and Development.
- Kramer, S. L. (1996). *Geotechnical Earthquake Engineering*. New Jersey: Prentice Hall inc Upper Saddle River.
- Namikawa, T., Koseki, J., & Suzuki, Y. (2007). Finite element analysis of Lattice-Shaped ground improvement by Cement-Mixing for liquefaction mitigation. *Soils and Foundations*, 47(3), 559–576. <https://doi.org/10.3208/sandf.47.559>

- Nguyen, T. V., Rayamajhi, D., Boulanger, R. W., Ashford, S. A., Lu, J., Elgamal, A., & Shao, L. (2013). Design of DSM grids for liquefaction remediation. *Journal of Geotechnical and Geoenvironmental Engineering*, 139(11), 1923–1933. [https://doi.org/10.1061/\(asce\)gt.1943-5606.0000921](https://doi.org/10.1061/(asce)gt.1943-5606.0000921)
- Ziotopoulou, K., and Boulanger, R. W. (2016). “Plasticity modeling of liquefaction effects under sloping ground and irregular cyclic loading conditions.” *Soil Dynamics and Earthquake Engineering*, 84 (2016), 269-283, 10.1016/j.soildyn.2016.02.013.
- Ziotopoulou, K., and Boulanger, R. W. (2013). “Calibration and implementation of a sand plasticity plane-strain model for earthquake engineering applications.” *Journal of Soil Dynamics and Earthquake Engineering*, 53, 268-280, 10.1016/j.soildyn.2013.07.009.